

$4f(^1P)$ Giant Dipole Resonance in La^{3+}

U. Köble, L. Kiernan, J. T. Costello, J-P. Mosnier, and E. T. Kennedy
Dublin City University, School of Physical Sciences, Dublin 9, Ireland

V. K. Ivanov, V. A. Kupchenko, and M. S. Shendrik
St. Petersburg Technical University, St. Petersburg, Russia
(Received 11 May 1994)

Photoabsorption of free La^{3+} ions in the $4d$ excitation region has been measured using the dual-laser plasma technique. A dramatic strong and broad $4d^9 4f(^1P)$ giant dipole resonance was observed. The interpretation of the results is provided using theoretical techniques which go beyond the independent particle approximation. In particular the strong term dependence for $4f(^1P)$ gives evidence of strong polarization effects for the description of the giant dipole resonance.

PACS numbers: 32.30.Jc, 32.70.Cs, 32.80.Dz

Giant resonances appear in the spectra of atoms, molecules, and solids as strong, broad, and asymmetric features [1]. Their existence arises from their multiparticle nature which is of general interest in the study of many-body effects. Very recently a giant plasmon resonance in fullerene C_{60} has been measured [2], where many-body calculations utilizing the random phase approximation (RPA) predicted a resonance with tremendous oscillator strength [3].

The importance of atomic systems for the study of many-body theories arises because of their relatively simple structure and because the electromagnetic interaction between the constituents of the many particle system is well known. A prominent example is the $4d$ giant dipole resonance in Ba and La which has been extensively discussed within different many-body theories [4–7]. Recent experimental studies of the decay channels of atomic [8,9] and metallic La [10] in the VUV excitation region display the continuing interest in this topic. Theorists have also focused on the $4d$ inner-shell photoexcitation of neutral, singly, or multiply ionized atoms along the Ba [11] and La isonuclear [12] sequence and the XeI isoelectronic [13,14] sequence in order to gain further insight into fundamental aspects such as electron-correlation effects, centrifugal barrier effects, and orbital collapse in term dependent Hartree-Fock potentials.

However, very little is known experimentally on photoexcitation processes for ionic species due to the severe experimental difficulties inherent in production of a sufficiently dense ion column. Only very few cross section measurements for ions are available to date for comparison with theory. In fact, the classic experimental results for Ba, Ba^+ , and Ba^{2+} by Lucatorto *et al.* [15] remain the only existing data for an extended isonuclear sequence in the giant resonance energy region. A dramatic change in the photoabsorption behavior in moving along the isonuclear sequence between Ba^+ and Ba^{2+} was observed. This led to considerable discussion in the literature (see [1] and contributions therein). Further calculations for ions in the

XeI isoelectronic sequence [13,14] predicted that in moving from Ba^{2+} to its isoelectronic partner La^{3+} the gradual orbital collapse in the 1P channel should lead to the $4d^9 4f(^1P)$ resonance becoming the dominant photoabsorption feature.

In order to test their prediction the XeI isoelectronic sequence was extended beyond Ba^{2+} to La^{3+} with the use of the dual-laser plasma (DLP) technique [16]. While the photographically recorded photoabsorption spectrum showed absorption lines successfully assigned to La^{3+} the $4d^9 4f(^1P)$ resonance was *not* observed. Further insight into the orbital collapse phenomenon was provided, in that calculations [16] showed that the increase of oscillator strength occurs concomitantly with a strong broadening of the resonance line. A very recent calculation for the $4d \rightarrow 4f$ transition for Ce^{4+} [17] supports this contention.

In this Letter we report for the first time photoelectric based photoabsorption cross section data for Ba^{2+} and La^{3+} , which enable us to provide a critical comparison between experimental results and predictions based on configuration interaction Hartree-Fock (CI-HF) and many-body perturbation techniques.

In the previous experiment [16] a single laser beam was optically split to create two plasmas and photographic detection was employed. The present experiment contains a number of very significant improvements. A Nd:YAG laser (1 J, 10 ns pulse) was used to produce a more intense and shorter duration continuum backlighting pulse. A second laser (ruby, 1.5 J, 30 ns pulse) enabled us to produce a longer path length (1.2 cm) in the absorbing plasma due to the fact that more laser energy was now available. These improvements, coupled with the use of a toroidal mirror which imaged the transmitted light into the spectrometer and a multichannel photoelectric detector with a linear response and good dynamic range, provided single shot sensitivity and allowed spatially and temporally resolved spectra to be obtained in a reproducible manner. By varying the irradiance conditions on the absorber target, its position relative to the optical axis and

the interlaser time delay, time and space resolved photoabsorption spectroscopy of the absorption plasma was achieved. In order to obtain relative cross sections, spectra were recorded with (I) and without (I_0) the absorbing plasma. The natural logarithm of the ratio (I_0/I) yielded the absorption data presented here.

Figure 1 shows the relative photoabsorption cross section data for the Ba^{2+} and La^{3+} isoelectronic pair obtained with an instrumental resolving power of ~ 1000 . The direct comparison shows a striking change in the photoabsorption behavior. Most impressive for La^{3+} is the strong and broad resonance at the photon energy of 118.9 eV which is the predicted dominant $4d^9 4f(^1P)$ term and the reduction in the continuum absorption background. The triplet state $4d^9 4f(^3D)$ [16] is also clearly recognizable at 102.1 eV.

The $4d^9 5s^2 5p^6 4f^1$ configuration of La^{3+} has been studied previously by Hansen [18] using HF calculations. He showed strong LS -term dependence (LSD) among the $J = 1$ levels due to the influence of the large $G^1(d, f)$ integral on the 1P term. We therefore performed LSD-HF calculations with the suite of the Cowan codes [19] in which the procedure is to minimize the energy of the

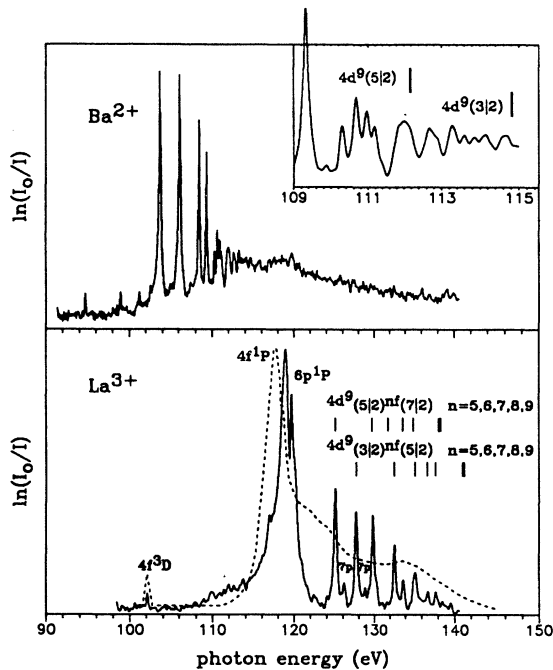


FIG. 1. Photoabsorption spectra of Ba^{2+} and La^{3+} in the $4d$ excitation region using the dual-laser plasma (DLP) technique. The enlarged Ba^{2+} spectrum shows the $4d_{(5/2),(3/2)}^9 n f$ Rydberg series for $n = 9, \dots, 12$, where the states with the $4d_{(3/2)}^9$ hole lie above the $4d_{(5/2)}^9$ threshold. The thresholds deduced from the experimental data are 112.2 ± 0.2 and 114.8 ± 0.2 eV, which agree well with the values given in [24]. The La^{3+} spectrum is shown together with photoabsorption data of solid LaF_3 from Ref. [23]. The thresholds $4d_{(5/2),(3/2)}^9$ deduced from the experimental data of La^{3+} are 138.2 ± 0.2 and 141.1 ± 0.2 eV.

term in question instead of the center of gravity (c.g.) of the configuration. This results in different potentials for the triplet and singlet states as illustrated for the appropriate wave functions $4f(^3D_1)$ and $4f(^1P_1)$ in the upper part of Fig. 2. Relaxation effects were included in the computation of the HF orbitals (see Cowan [19], Sect. 13.2); this proves essential when a comparison is made with many-body-type calculations presented later. The obtained energy value for the $4f(^1P_1)$ is 121.3 eV (see Fig. 2, lower part) which can be compared with the previous results of 123.8 eV by Hansen [18] and 121.2 eV by Starace [20].

In a more illustrative picture, the term dependence of the excited $4f$ state can be interpreted as a departure from the original spherical symmetry of the electron distribution. This is caused by the rearrangement processes of the remaining $4d$ electrons in response to the excitation which leads to a new dipole symmetry. The consequent polarization, which is considered here to be an important effect, can be taken into account in a c.g. HF calculation, in an intermediate coupling scheme, including extended $4d^9(n, \epsilon)f$ configuration interactions. This calculational approach was taken by Hansen *et al.* [16] where $4d \rightarrow$

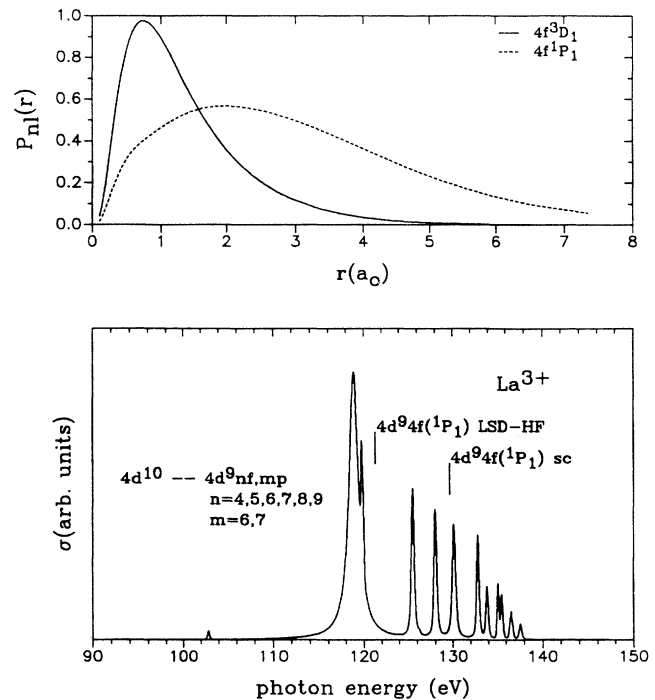


FIG. 2. Upper part: $4f(^3D_1)$ and $4f(^1P_1)$ wave functions of La^{3+} . The large difference illustrates the strong term dependence for the 1P state. Lower part: Calculated photoabsorption spectrum in the $4d$ excitation region for La^{3+} with the CI-HF method. The spectrum is convolved with a Gaussian profile of 0.15 eV width for comparison with the experimental data. The vertical bars represent the energies of the $4d^9 4f(^1P)$ term calculated via single configuration center of gravity (sc) Hartree-Fock and LS term dependent Hartree-Fock method.

$(n, \epsilon)f$ intrachannel CI-HF calculations including the $6p$ and $7p$ states were performed. Their *ab initio* results are in fairly good agreement with the new experimental data but cannot explain the observed splitting of the main peak.

Using a similar CI-HF approach to Hansen *et al.* [16] we scaled the G^k Slater integrals by a factor of 0.82 in order to shift the $4f(^1P)$ term down to its observed position from 120.9 to 118.9 eV. Since only the $4f(^1P)$ term is largely influenced by the G^1 integral, the scaling has negligible effects on the energy positions of the other terms. The new position of the $4d^9 4f(^1P)$ state is now much closer to the $4d^9_{3/2} 6p_{1/2}$ state, which affects the mixing of these states after the diagonalization of the CI energy matrix, and the latter one gains distinctly in oscillator strength and autoionization width. As a result we obtained an f value, calculated in the length form, of 5.0 for the $4d^9 4f(^1P)$ and 0.22 for the $4d^9_{3/2} 6p_{1/2}$ states. The results of the new calculation enable us to assign the observed transition lines to members of the Rydberg series converging to their appropriate $4d^9_{(5/2),(3/2)}$ limits as shown in Fig. 1.

We have estimated the autoionizing widths of the resonance lines using the R^k integrals connecting the eigenvector components of the diagonalized energy matrix to the $5s^2 5p^{-1} \epsilon(s, d)$ and $5s^1 5p^0 \epsilon p$ continua. Since the asymmetry parameter q is very large, the shapes of the resonance lines were approximated by Lorentzian profiles $f\Gamma\pi^{-1}/[(E - E_0)^2 + \Gamma^2]$ with E_0 the peak energy and 2Γ the FWHM of the resonance line. Figure 2 (lower part) shows the calculated spectrum convolved with a Gaussian profile of 0.15 eV width in order to take the instrumental resolution into account. Good agreement with the experimental data in Fig. 1 is achieved for the $4d^9 nf$ Rydberg states and the $4d^9 6p$ lines, while the $4d^9 7p$ lines seem to be underestimated.

In the discussion so far, the many electron response to the external field is accounted for by an effective one electron wave function $4f(^1P)$ which is used in the calculations of the transition and electrostatic interaction matrix elements. An alternative approach is to consider that the external field polarizes the electron charge cloud of the atom which gives rise to an induced field. Both external and induced fields superimpose to produce an effective driving field to which the electrons respond independently. In this sense, when the external field is rather weak, the random phase approximation with exchange (RPAE) can be regarded as a time dependent effective mean field theory. We have calculated the La^{3+} spectrum using the RPAE in conjunction with the many-body perturbation theory (MBPT) over the whole photon energy region of interest. The MBPT starts from the HF approximation (HFA) as a zero one, where the $4d$ subshell energy was obtained to be -146.49 eV and the $4d \rightarrow 4f$ transition energy 125.75 eV. The $4d$ spin-orbit splitting was calculated within first order perturbation theory to be 2.85 eV. We thus obtain the following

energies: $E_{4d_{5/2}} = -145.35$ eV and $E_{4d_{3/2}} = -148.20$ eV. To improve the transition energy, we go beyond the HFA by calculating the self-energy part $\Sigma_{4d}(E)$ of the single electron Green's function for the $4d$ electron within second order perturbation theory [21]. The new energy of the $4d$ subshell corrected due to the many electron interaction is obtained by solving the equation $E_{4d} = E_{4d}^{\text{HF}} + \text{Re}\langle 4d | \Sigma(E_{4d}) | 4d \rangle$ self-consistently. As a result, the E_{4d} energy shift is calculated to be 4.56 eV and the corrected $4d$ subshell energy -141.9 eV. The imaginary part of $\langle \Sigma(E_{4d}) \rangle$ determines the width of the $4d$ hole state due to Auger decay, $\gamma_A = 0.059$ eV.

The oscillator strengths of the discrete transitions are calculated within the RPAE, where the five dipole channels $5p \rightarrow \epsilon(s, d)$; $5s \rightarrow \epsilon p$ and $4d \rightarrow (n, \epsilon)(p, f)$ are taken into account. The main contribution comes from the $4d \rightarrow 4f$ transition, which reveals itself as a giant autoionizing resonance with a FWHM $2\Gamma = 1.15$ eV and an oscillator strength of 6.37. The results of the corrected energies, oscillator strengths, and width (Auger and autoionization) for the $4d \rightarrow nf, mp$ transitions with $n = 4, 5, \dots, 8$ and $m = 6, 7, 8, 9$ are represented in Fig. 3. The comparison with the experimental data confirms the assignment of the two strong resonance lines at 118.95 and 119.70 eV due to $4d_{5/2} \rightarrow 4f, 6p$ transitions. It has been shown that in cases of the interaction between a broad giant resonance and a Rydberg series of finer structures the latter often appear as window resonances [22]. Our calculations indicate that the q parameter for the $4d \rightarrow 6p$ profile is significantly larger than 1 which argues against a window resonance interpretation in this case.

The predicted series $4d_{3/2} \rightarrow 4f, 6p$ between 121 and 123 eV (see Fig. 3) is not observed in the experiment (Fig. 1). This may be connected with a redistribution of oscillator strengths due to strong coupling between the $4d_{5/2, 3/2} \rightarrow 4f$ transitions via the effective mean field, which is considered to be important for overlapping resonances with large width, but has not been taken into account here [6]. Strong mean field coupling causes the spin-orbit split subshells to oscillate in two modes: in phase acting like a single subshell with a large oscillator

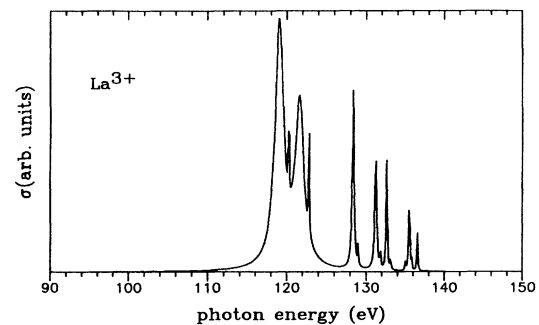


FIG. 3. Calculated photoabsorption spectrum in the $4d$ excitation region of La^{3+} with the method of the MBPT and RPAE.

strength and out of phase leading to near cancellation of the induced fields with a weak oscillator strength and a negligible energy shift. However, for the higher transition series, where the widths are significantly smaller, spin-orbit splitting becomes dominant, and we obtain spin-orbit split transitions with relative intensities in the ratio of the statistical weights.

Apart from their fundamental theoretical interest, photoabsorption cross sections of free ions also provide key data for the understanding of the electronic structure of solids and molecules. In order to illustrate this point, we compare our experimental data in Fig. 1 (lower part) with the corresponding photoabsorption cross sections of solid LaF_3 presented in Ref. [23]. Both spectra show the dominant $4d^9 4f(^1P)$ resonance and the weak $4f(^3D)$ line at about 102 eV. The shoulder at 118.8 eV in the solid state spectrum corresponds to the $4d_{(3/2)}^9 6p_{(1/2)}$ state in La^{3+} . The comparison of both spectra shows that the $4f(^1P)$ resonance of La^{3+} in its solid state is actually influenced albeit moderately by the environment, which causes the resonance to be broadened and shifted by about 1.3 eV toward lower energy. The 4d excitations into higher levels are also recognizable in the LaF_3 spectrum. However, in these cases the disappearance of the pronounced line structure that prevails in the free ion spectrum is a clear indication of the nonlocalized character of these states.

In conclusion, we have shown that the giant dipole resonance in La^{3+} associated with the 4d subshell excitation has acquired a definite discrete $4d^{10} \rightarrow 4d^9 4f(^1P)$ character at the expense of the $4d^{10} \rightarrow 4d^9 \epsilon f$ continuum transitions. Polarization effects revealed through a large term dependence of the $4f(^1P)$ state are found to be strong. Comparison with the corresponding spectrum of Ba^{2+} confirms the theory which predicts that the collapse of the $4f^1 P$ orbital along the XeI sequence has a gradual nature and is not yet complete for Ba^{2+} . Finally, the giant dipole resonance in La^{3+} remains essentially unaffected by a solid state environment such as LaF_3 .

We wish to acknowledge the support of Michael Martins in some of the computational aspects. This research was supported by the European Community under Contract No. SCI0364, EOLAS under Contracts No. SC91/120 and No. SC93/144, and also the BMFT/EOLAS under the German-Irish cooperation scheme.

- [1] *Giant Resonances in Atoms, Molecules, and Solids*, edited by J.P. Connerade, J.M. Estava, and R.C. Karnatak (Plenum Press, New York, 1987), and references therein.
- [2] I. V. Hertel, H. Steger, J. de Vries, B. Weisser, C. Menzel, B. Kamke, and W. Kamke, Phys. Rev. Lett. **68**, 784 (1992).
- [3] G.F. Bertsch, A. Bulgac, D. Tománek, and Y. Wang, Phys. Rev. Lett. **67**, 2690 (1991).
- [4] G. Wendin, Phys. Lett. **46A**, 119 (1973).
- [5] M. Ya. Amusia and S.I. Sheftel, Phys. Lett. **55A**, 469 (1976).
- [6] G. Wendin, *New Trends in Atomic Physics*, edited by G. Grynberg and R. Stora (Elsevier Science Publishers BV, New York, 1984), p. 555.
- [7] A. Zangwill and P. Soven, Phys. Rev. Lett. **45**, 204 (1980).
- [8] Ch. Dzionk, W. Fiedler, M. van Lucke, and P. Zimmermann, Phys. Rev. Lett. **62**, 878 (1989).
- [9] M. Richter, M. Meyer, M. Pähler, T. Prescher, E. von Raven, B. Sonntag, and H.E. Wetzel, Phys. Rev. A **39**, 5666 (1989).
- [10] O-P. Sairanen, S. Aksela, and A. Kivimäki, J. Phys. Condens. Matter **3**, 8707 (1991).
- [11] K. Nuroh, M.J. Stott, and E. Zaremba, Phys. Rev. Lett. **49**, 862 (1982).
- [12] M. Ya. Amusia, V.K. Ivanov, V.A. Kupchenko, and L.V. Chernysheva, Z. Phys. D **14**, 215 (1989).
- [13] K.T. Cheng and C. Froese Fischer, Phys. Rev. A **28**, 2811 (1983).
- [14] K.T. Cheng and W.R. Johnson, Phys. Rev. A **28**, 2820 (1983).
- [15] T.B. Lucatorto, T.J. McIlrath, J. Sugar, and S.M. Younger, Phys. Rev. Lett. **47**, 1124 (1981).
- [16] J.E. Hansen, J. Brilly, E.T. Kennedy, and G. O'Sullivan, Phys. Rev. Lett. **63**, 1934 (1989).
- [17] V. Ivanov, in *Proceedings of the 10th VUV Conference, Paris, 1992*, edited by F.J. Wuilleumier, Y. Petroff, and I. Nenner (World Scientific, Singapore, 1993), p. 178.
- [18] J.E. Hansen, J. Phys. B **5**, 1096 (1972).
- [19] R.D. Cowan, *The Theory of Atomic Structure and Spectra* (University of California Press, Berkeley, 1981).
- [20] A.F. Starace, J. Phys. B **7**, 14 (1974).
- [21] M. Ya. Amusia, *Atomic Photoeffect* (Plenum Press, New York, 1990).
- [22] J.P. Connerade and A.M. Lane, J. Phys. B **20**, L181 (1987).
- [23] C.G. Olsen and D.W. Lynch, J. Opt. Soc. Am. **72**, 88 (1982).
- [24] C.W. Clark, J. Opt. Soc. Am. B **1**, 626 (1984).